Phys Chem Minerals (2013) 40:479–489
DOI 10.1007/s00269-013-0585-5

ORIGINAL PAPER

Studies on the solid acidity of heated and cation-exchanged montmorillonite using *n*-butylamine titration in non-aqueous system and diffuse reflectance Fourier transform infrared (DRIFT) spectroscopy

Hongmei Liu · Dong Liu · Peng Yuan · Daoyong Tan · Jingong Cai · Hongping He · Jianxi Zhu · Zhiguang Song

Received: 20 August 2012 / Accepted: 13 March 2013 / Published online: 31 March 2013

Abstract The effects of heating and cation exchange on the solid acidity of montmorillonite were investigated using *n*-butylamine titration in non-aqueous system and diffuse reflectance Fourier transform infrared spectroscopy. The number of total, Brønsted, and Lewis acid sites showed the same modulation tendency with increasing heating temperature, reaching a maximum at 120 °C and subsequently decreasing until it reaches a minimum at 600 °C. The Lewis acid sites result from unsaturated Al^{3+} cations, and their number increased with the heating temperature due to the dehydration and dehydroxylation of montmorillonite. The generation and evolution of Brønsted acidity were mainly related to interlayer-polarized water molecules. Water adsorbed on the unsaturated Al^{3+} ions also acted as a Brønsted acid. The acid strength of the Brønsted acid sites was dependent on the polarization ability of the exchangeable cation, the amount of interlayer water, and the degree of dissociation of the interlayer water coordinated to exchangeable cations. All cation-exchanged montmorillonites exhibited different numbers of acid sites and various distributions of acid strength. Brønsted acidity was predominant in Al^{3+}-exchanged montmorillonite, whereas the Na^{+}- and K^{+}-exchanged montmorillonites showed predominantly Lewis acidity. Moreover, Mg^{2+}- and Li^{+}-exchanged montmorillonites exhibited approximately equal numbers of Brønsted and Lewis acid sites. The Brønsted acidity of cation-exchanged montmorillonite was positively correlated with the charge-to-radius ratios of the cations, whereas the Lewis acidity was highly dependent on the electronegativity of the cations. The acid strengths of Al^{3+}- and Mg^{2+}-exchanged montmorillonites were remarkably higher than those of monovalent cation-exchanged montmorillonites, showing the highest acid strength ($H_0 \leq -3.0$). Li^{+}- and Na^{+}-exchanged montmorillonites exhibited an acid strength distribution of $-3.0 < H_0 \leq 4.8$, with the acid strength ranging primarily from 1.5 to 3.3 in Li^{+}-exchanged montmorillonite, whereas only weaker-strength acid sites ($1.5 < H_0 \leq 4.8$) were present in K^{+}-exchanged montmorillonite. The results of the catalysis experiments indicated that montmorillonite promoted the thermal decomposition of the model organic. The catalytic activity showed a positive correlation with the solid acidity of montmorillonite and was affected by cation exchange, which occurs naturally in geological processes.

Keywords Solid acidity · Montmorillonite · Heating · Cation exchange · Non-aqueous titration · DRIFT

Electronic supplementary material The online version of this article (doi:10.1007/s00269-013-0585-5) contains supplementary material, which is available to authorized users.

H. Liu · D. Liu · P. Yuan (✉) · D. Tan · H. He · J. Zhu
CAS Key Laboratory of Mineralogy and Metallogeny, Guangzhou Institute of Geochemistry, Chinese Academy of Sciences, Guangzhou 510640, China
e-mail: YuanPeng@GIG.ac.Cn

H. Liu · D. Tan
University of Chinese Academy of Sciences, Beijing 100049, China

J. Cai
School of Ocean and Earth Science, Tongji University, Shanghai 200092, China

Z. Song
The State Key Laboratory of Organic Geochemistry, Guangzhou Institute of Geochemistry, Chinese Academy of Sciences, Guangzhou 510640, China

Introduction

Montmorillonite is a raw clay mineral with a dioctahedral 2:1 layered structure. It is widely used as a catalyst, a catalytic support, and an adsorbent due to its high cation-exchange capacity and large surface area, excellent adsorption and swelling properties, and solid acidity (Vaccari 1999; Varma 2002; Zhou 2011). Brønsted and Lewis acid sites coexist in the structure of montmorillonite and offer a wide range of applications in organic reactions, in which a high acid-type selectivity is required (Adams and McCabe 2006; Motokura et al. 2007; Reddy et al. 2007; Singh et al. 2007; Shimizu et al. 2008). Moreover, the inherent solid acidity of montmorillonite is also well known to be significant in geological processes, such as the generation of kerogens (Johns and Shimoyama 1972; Larter and Douglas 1982; Heténi 1995; Geatches et al. 2010) and the catalytic formation of hydrocarbons.

Various methods have been proposed for the determination of solid acid amount and differentiation of Brønsted and Lewis acid sites in montmorillonite. The Hammett indicators technique (Walling 1950; Benesi 1957; Adams and McCabe 2006; Liu et al. 2011), *n*-butylamine back titration (Reddy et al. 2005), and microcalorimetry (Breen 1991a, b; Hart and Brown 2004; Jerónimo et al. 2007) have been used to determine the number of acid sites. The temperature-programmed desorption of basic gas molecules (Arena et al. 1998; Breen et al. 1987; Adams and McCabe 2006; Singh et al. 2007) and Hammett indicators (Walling 1950; Benesi 1957; Liu et al. 2011) have been used to evaluate the strength of acid sites. In addition, Brønsted and Lewis acid sites can be distinguished by differentiating vibrational bands of the adsorbed basic probe molecules using Fourier transform infrared spectroscopy (FTIR) (Akçay 2005; Billingham et al. 1996; Brown and Rhodes 1997; Cseri et al. 1995; Flessner et al. 2001; Liu et al. 2011; Reddy et al. 2009; Reddy et al. 2007; Singh et al. 2007; Tyagi et al. 2006). Based on these investigations, the number of acid sites in montmorillonite obtained from different sources has been found to range from 0.09 to 0.60 mmol/g (Flessner et al. 2001; Hart and Brown 2004; Liu et al. 2011; Walling 1950). However, the solid acidity of montmorillonite is difficult to compare directly between different studies because both the samples used and the applied measurement methods are not uniform. Moreover, only one or two, rather than all solid acidity parameters, were determined in the above reports. Therefore, a complete evaluation of the solid acidity of montmorillonite, including the types and origins of solid acid sites, the acid amount, and the distribution of acid strength, is necessary. The solid acidity of montmorillonite is greatly influenced by heating and cation-exchange processes (Billingham et al. 1996; Brown and Rhodes 1997; Heller-Kallai 2006; Liu et al. 2011; Noyan et al. 2006; Reddy et al. 2009; Reddy et al. 2007). However, most investigations have focused on acid-activated montmorillonite due to its high acidity and excellent performance in catalytic reactions, such as Friedel–Crafts alkylation and the polymerization of unsaturated hydrocarbons. Less attention has been given to the solid acidity of heated and cation-exchanged montmorillonite. In fact, cation-exchanged montmorillonite is of particular significance for geological processes based on the geocatalysis of clay minerals because montmorillonite in natural diagenesis is usually exposed to a cationic (e.g., Al^{3+}, Mg^{2+}, Li^{+}, Na^{+}, and K^{+}) environment at high temperatures (Bjølykke 1998; Fripiat and Cruz-Cumplido 1974; Johns 1979; Johns and Shimoyama 1972).

The main objective of the present work was to better understand how the solid acidity of montmorillonite changes after heat and cation-exchange treatment. For a complete evaluation of the solid acidity, a combined technique using *n*-butylamine titration in non-aqueous system and diffuse reflectance Fourier transform infrared (DRIFT) spectroscopy was applied to detect the total number and strength of the solid acid sites and to distinguish the types of solid acid sites by using pyridine as a probe molecule. To evaluate the catalytic activity of cation-exchanged montmorillonite with different solid acidities in hydrocarbon generation, thermal decomposition experiments of typical organic matter were conducted in the presence of montmorillonite. 12-aminolauric acid (ALA; $NH_2(CH_2)_{11}COOH$) was selected as the organic model because it contains some common functional groups of natural organics, such as amino and carboxyl groups, and represents some types of natural organics (Wattel-Koekkoek et al. 2001). The catalytic activity was investigated by the thermal decomposition temperature of ALA, which was obtained by thermogravimetric (TG) and derivative TG (DTG) analysis.

Materials and methods

Materials

Ca-montmorillonite from Inner Mongolia, China, supplied by Wu Hua Tian Bao Mining Ltd., was purified using a conventional sedimentation method. The <2 μm fraction was collected and dried at 60 °C. The chemical compositions (wt%) of montmorillonite (denoted as Mt) were as follows: SiO_2 58.16 %, Al_2O_3 16.95 %, Fe_2O_3 5.26 %, CaO 2.29 %, MgO 3.57 %, Na_2O 0.19 %, K_2O 0.15 %, MnO 0.03 %, TiO_2 0.20 %, P_2O_5 0.08 %, and the ignition loss 13.12 %. The cation-exchange capacity was 110.5 mmol/100 g (see Supplementary Information (SI)).

Thermally treated samples were obtained by heating Mt in a programmed temperature-controlled muffle oven at 120, 200, 400, and 600 °C for 3 h; the obtained samples

were ground in an agate mortar and denoted as Mt-120, Mt-200, Mt-400, and Mt-600, respectively.

Cation-exchanged montmorillonite was prepared as follows: 10 g Mt was dispersed in 200 mL of a 0.5 M salt solution of chloride containing the desired cations under vigorous stirring at 80 °C for 24 h. The clay was then separated from the solution and treated with a fresh salt solution, followed by two repetitions of the cation-exchange procedure for complete exchange. The resulting mixture was centrifuged and washed by successive centrifugations with deionized water until no chloride was detected with an $AgNO_3$ solution. Then, all of the prepared samples were dried initially at 60 °C and subsequently ground to a fine powder, followed by heating at 120 °C for 3 h; these samples were denoted as Na^+-Mt, K^+-Mt, Li^+-Mt, Mg^{2+}-Mt, and Al^{3+}-Mt. All samples were kept in a desiccator for further use.

Methods and characterization

Acidity measurement

The *n*-butylamine titration using Hammett indicators was used to measure the number of solid acid sites and the acid strength distribution of the samples following the classic procedure reported in the literature (Benesi 1957; Liu et al. 2011). The details of the experiment are provided in the SI, and the Hammett indicators used in this study are listed in Table S1 (see SI).

Pyridine was used as a basic probe molecule of DRIFT to distinguish the Brønsted and Lewis acid sites of the samples. Before measurement, the samples were directly treated with pyridine in a desiccator for 7 days. Subsequently, the samples were evacuated for 10 min at room temperature to remove the physically adsorbed pyridine. The resulting pyridine-adsorbed samples were differentiated by postfixing the sample names with "/Py". For example, Mt-200/Py denotes a montmorillonite sample heated to 200 °C with the further adsorption of pyridine.

Thermal decomposition experiment

Experiments on the thermal decomposition of ALA were performed as follows. A total of 10.0 g of cation-exchanged montmorillonite was mixed with 2.5 g of ALA by ball milling for 20 min using a Pulverisette-6 Planetary Mill. Thermal decomposition temperatures of ALA in the absence and presence of cation-exchanged montmorillonite were measured using TG analysis.

Characterization

The TG analysis was performed on a Netzsch 449C instrument. Approximately 20 mg of each finely powdered sample was heated from 30 to 1,000 °C at a heating rate of 10 °C/min under a highly pure N_2 atmosphere (60 cm^3/min).

The X-ray diffraction (XRD) patterns of the samples were recorded on a Bruker D8 Advance diffractometer with a Ni filter and CuKα radiation ($\lambda = 0.154$ nm) using a generator voltage of 40 kV and a generator current of 40 mA; a scan rate of 1° (2θ)/min was applied for the analysis.

DRIFT spectra were obtained using the Praying Mantis™ diffuse reflection accessory of a Bruker Vertex-70 Fourier transform infrared spectrometer at room temperature. The spectra were collected over the range of 600–4,000/cm with 64 scans at a resolution of 4/cm, using KBr as the background.

Results and discussion

Influences of heating and cation exchange on the structure of montmorillonite

Two mass losses are resolved in the TG curve (Fig. 1a) of Mt. The mass loss in the range of 30–200 °C, with the corresponding derivative DTG peaks centered at 133 and 177 °C, is attributed to the desorption of the surface-adsorbed water and interlayer water of Mt (He et al. 2006; Heller-Kallai 2006). The second mass loss occurred between 500 and 700 °C, with the maximum mass loss rate occurring at approximately 633 °C, corresponding to the dehydroxylation of Mt.

Figure 2a shows the XRD patterns of Mt and its heated products. In the XRD pattern of Mt, the sharp reflection at approximately 6° ($d = 1.47$ nm) is attributed to a (001) reflection, and the weak peak at approximately 27° ($d = 3.33$ nm) corresponds to the diffraction of a quartz (denoted as Q in Fig. 2) impurity. The quartz content was semiquantitatively determined to be 3 %. The XRD patterns of Mt and its heated products show that the $d_{(001)}$ value and the intensity of the corresponding peak decrease with increasing heating temperature. The $d_{(001)}$ values of Mt-120 and Mt-200 are 1.46 and 1.43 nm, respectively. These values are slightly smaller than the value of Mt, which indicates the partial removal of the interlayer water after heating at low temperatures (≤200 °C). However, Mt-400 exhibits a clearly reduced $d_{(001)}$ value (0.98 nm) and a broad (001) reflection, indicating the removal of most of the interlayer water. Mt-600 exhibits the lowest $d_{(001)}$ value (0.97 nm), and the interlayer distance is ~0.01 nm based on the thickness of the dehydrated montmorillonite, ~0.96 nm (Khaorapapong et al. 2008). This weak and broad (001) reflection of Mt-600 implies the collapse of the interlayer space due to the complete dehydration and partial removal of hydroxyl groups (Heller-Kallai 2006; Ursu

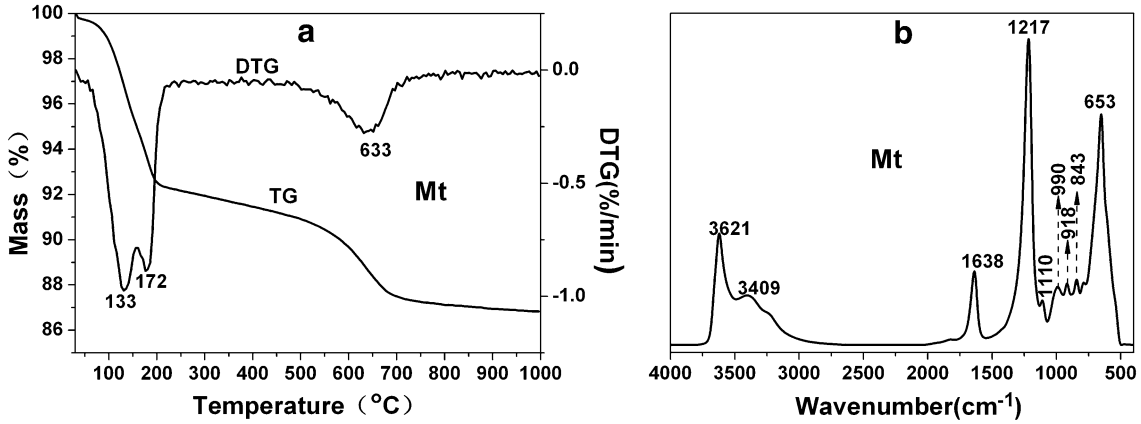

Fig. 1 TG and DTG curves of Mt (**a**), DRIFT spectrum of Mt (**b**)

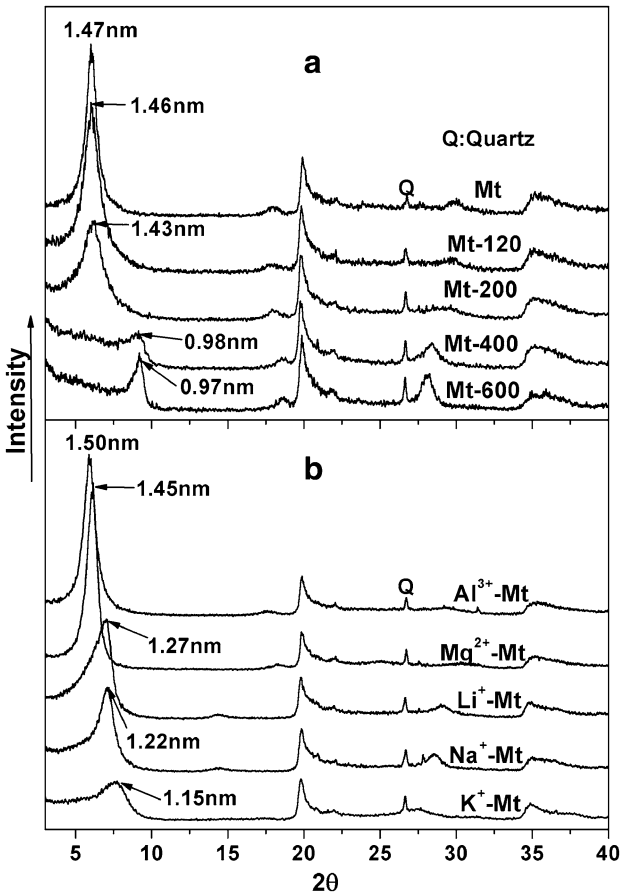

Fig. 2 XRD patterns of Mt and its heated products (**a**), cation-exchanged products (**b**)

et al. 2011). This result is consistent with that of the TG analysis.

As shown in Fig. 2b, the $d_{(001)}$ values of cation-exchanged Mt are different from each other. Al^{3+}-Mt exhibits the largest $d_{(001)}$ value of 1.50 nm, and the corresponding $d_{(001)}$ values of Mg^{2+}-Mt, Li^{+}-Mt, Na^{+}-Mt, and K^{+}-Mt are 1.45, 1.27, 1.22, and 1.15 nm, respectively. As reported in the literature, monovalent cation-exchanged products with d-spacings ranging from approximately 1.2–1.3 nm are equivalent to one-layer hydrates. However, the $d_{(001)}$ values of Al^{3+}-Mt and Mg^{2+}-Mt indicate the presence of two layers of interlayer water in their interlayer space (Dontsova et al. 2004; Zheng et al. 2010), which suggests that the hydration characteristics of Mt strongly depend on the type of interlayer cation.

Figure 1b shows the DRIFT spectrum of Mt. The corresponding wave number and assignment of the main vibrational modes are summarized in Table S2, based on a previous report (Madejová and Komadel 2001) (see SI). The Si–O stretching band at 1,110/cm, which remains almost undisturbed after heating and cation exchange, is used as an internal standard to compare the relative area of the characteristic bands caused by the solid acidity of Mt and its heated and cation-exchanged products. After heating, changes are observed in the intensity of the adsorbed water vibrational bands (at ~3,409 and 1,638/cm) and structural hydroxyl group (–OH, at ~3,621/cm) in Mt (Fig. 3a). Among these changes, a decrease in the intensity of the vibrational bands of adsorbed water is observed with the increase in the heating temperature. These bands disappear after heating at 600 °C, indicating the complete dehydration of Mt. In contrast to that of adsorbed water, the intensity of structural –OH decreases significantly only after heating at 600 °C, implying the dehydroxylation of Mt. These results show good agreement with those of the TG and XRD experiments.

Notably, a similar intensity for the adsorbed water bands (~3,409 and 1,639/cm) appears in the spectra of the cation-exchanged products, except the K–Mt spectrum, which is weaker and broader. This result indicates a lower interlayer water content in K–Mt (Fig. 3c). A vibrational band at 1,217/cm appears in all DRIFT spectra, which might be

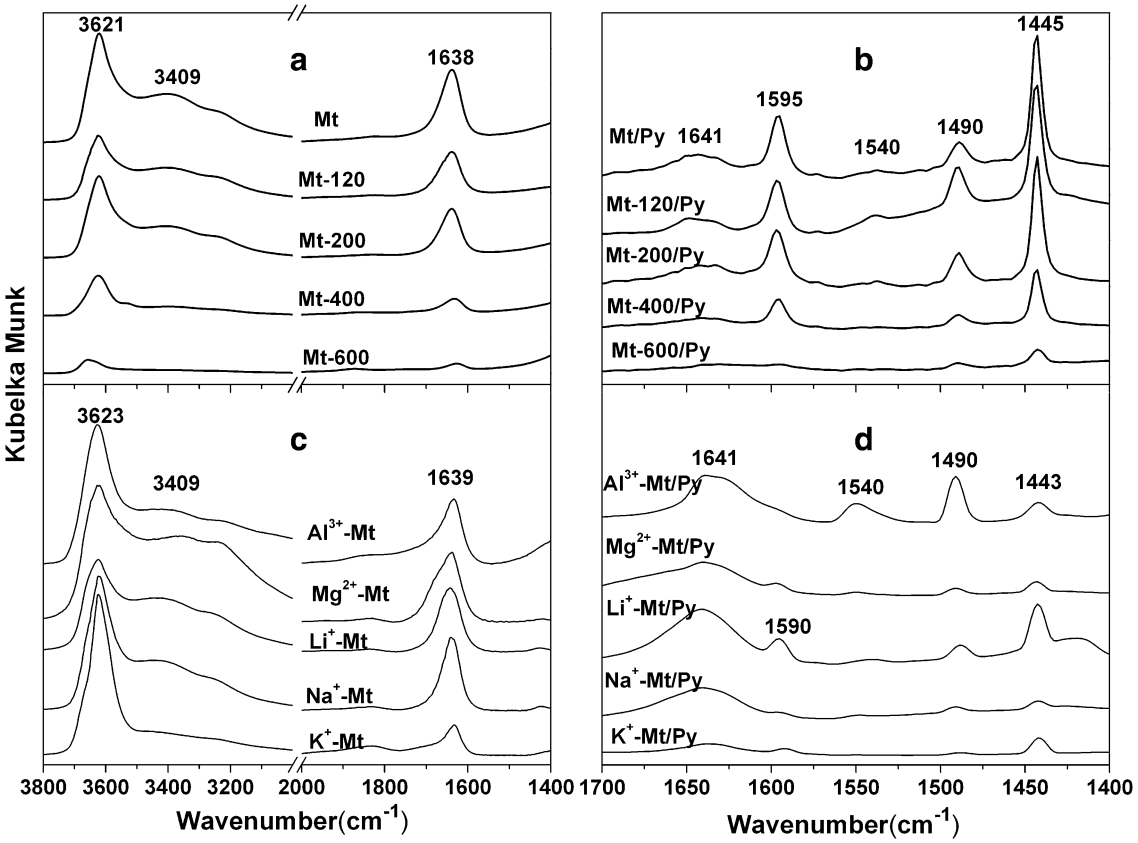

Fig. 3 DRIFT spectra of Mt and its heated and cation-exchanged products before (**a**, **c**) and after (**b**, **d**) pyridine adsorption

related to the perturbation of particular reflections and cannot provide any information about the samples (Madejová and Komadel 2001).

Acidity of heated and cation-exchanged montmorillonite

Acidity of heated montmorillonite

New vibrational bands (at 1,445, 1,490, 1,540, 1,595, and 1,641/cm) are observed in the 1,400–1,700/cm region of the DRIFT spectra of pyridine-adsorbed Mt (Fig. 3b). Except for the bands at ~1,540 and 1,641/cm, the other newly appeared bands are composed of two overlapping bands from the pyridine coordinated to the Lewis acid sites (denoted as L:Py), hydrogen-bound pyridine, and the pyridinium ion (PyH^+) (Table 1). The strong-intensity vibrational bands at ~1,445 and 1,595/cm are considered the overlapping band of L: Py and hydrogen-bonded pyridine, and the absorption band at 1,490/cm corresponds to the combination of the Brønsted and Lewis acid sites. The broad adsorption band at 1,641/cm is most likely due to the bending vibrations of the –OH group of residual water and some number of Brønsted (1,640/cm) and Lewis (1,620/cm) acid sites.

Table 1 Infrared bands of pyridine on acid solids in the 1,400–1,700/cm region (Breen et al. 1987; Brown and Rhodes 1997; Reddy et al. 2009)

Hydrogen-bonded pyridine	L:Py	PyH^+
1,440–1,447	1,447–1,460	
	1,488–1,503	1,485–1,500
		1,540
1,580–1,600	~1,580	
	1,600–1,633	1,620
		1,640

The 1,540, 1,490, and 1,450/cm bands are the most characteristic bands of Brønsted and Lewis acid sites (Jankovič and Komadel 2003). However, the precise intensities of the 1,445/cm band associated with the Lewis acid sites are difficult to estimate because of the overlaps of hydrogen-bonded pyridine. Assuming that the relative area of the band at 1,490/cm (denoted as A_T) is the sum of the relative areas of PyH^+ and L:Py (denoted as A_B and A_L), A_L can be obtained by subtracting A_B from A_T because A_T and A_B can be calculated using an internal standard method. A_B and A_L represent the relative numbers of

Brønsted and Lewis acid sites (denoted as Q_B and Q_L), respectively. Q_B is obtained from the following equation:

$$Q_B = Q_T \times \frac{A_B}{A_T} \times 100\ \% \quad (1)$$

Q_T is measured using *n*-butylamine titration in non-aqueous system, and Q_L is obtained by subtracting Q_B from Q_T (Table 2).

Mt has a considerable number of acid sites (0.80 mmol/g). With the rise in heating temperature, the Q_T of Mt increases first and then reduces gradually until it reaches a minimum at 600 °C (Fig. 4a). Mt-120 shows a maximum of 1.50 mmol/g, which is almost 10 times larger than that of Mt-600. The same trend is observed for Q_B and Q_L (Table 2). Q_B and Q_L are the highest at 120 °C (0.51 and 0.99 mmol/g, respectively) and reach their lowest values after heating at 600 °C. Mt-400 and Mt-600 exhibit rapid Q_T, Q_B, and Q_L reduction compared with the lower-temperature-heated samples. A similar trend in the number of acid sites was observed in our previous study (Liu et al. 2011). However, several different results have been obtained by other studies. For example, using a titration method, Mahmoud et al. (2003) found that the largest number of acid sites and the highest-strength acid sites appeared after heating at 250 °C on Jordanian bentonite, whereas Noyan et al. (2006) proposed that the acidity of bentonite declined with increasing temperature (from 25 to 900 °C) and found that the highest number of solid acid sites obtained was only 0.45 mmol/g, which is significantly lower than the value obtained in our study. The variation in these results is attributed to the specific features of different montmorillonite samples and the different acidity measurement methods used.

Table 2 Numbers of acid sites in Mt and its heated and cation-exchanged products (determined by *n*-butylamine titration in non-aqueous system)

Sample	Amounts of acid sites (mmol/g)		
	Q_T	Q_B	Q_L
Mt	0.80	0.26	0.54
Mt-120	1.50	0.51	0.99
Mt-200	0.95	0.29	0.66
Mt-400	0.33	0.10	0.23
Mt-600	0.16	0.08	0.08
Al^{3+}-Mt	1.20	0.91	0.29
Mg^{2+}-Mt	1.00	0.56	0.44
Li^{+}-Mt	0.65	0.27	0.38
Na^{+}-Mt	0.30	0.09	0.21
K^{+}-Mt	0.24	0.02	0.22

Lewis acidity is mostly associated with unsaturated Al^{3+} ions at the edge of the Mt layer (Rupert et al. 1987). The Q_L of Mt is 0.54 mmol/g and reaches its highest value at 120 °C. The increase in Q_L can be attributed to the exposure of some unsaturated Al^{3+} ions at the particle edges, which formerly absorbed water and exhibited Brønsted acidity (Rupert et al. 1987). The Q_L of Mt-400 decreased greatly, reaching values as low as 0.08 mmol/g at 600 °C. As mentioned in the literature, newly unsaturated Al^{3+} ions (Lewis acid sites) result from the rupture of Si–O–Al bonds or dehydroxylation at high temperatures (Bhattacharyya and Gupta 2008), and the Lewis acid sites that result from dehydroxylation are of significantly high acid strength

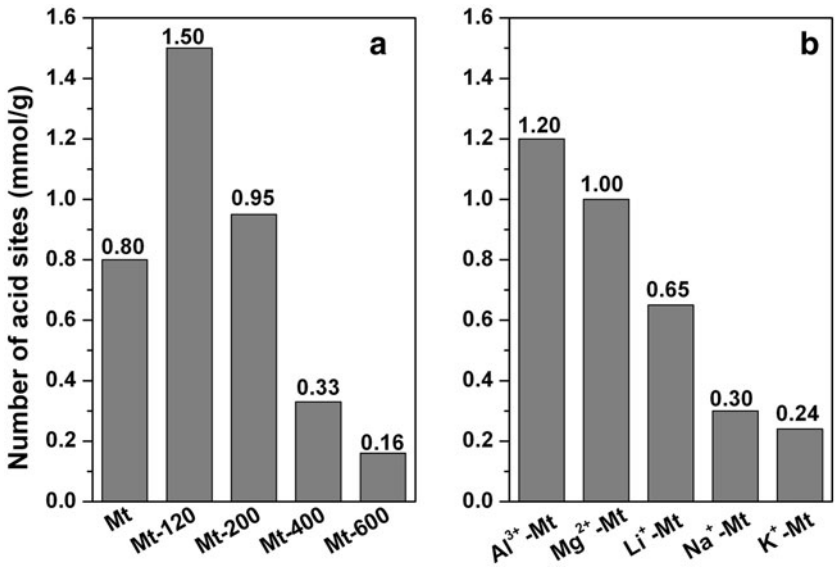

Fig. 4 The total number of acid sites of Mt and its heated (**a**) and cation-exchanged (**b**) products (determined by *n*-butylamine titration in non-aqueous system)

(Noyan et al. 2006). The abnormally low Q_L values of Mt-400 and Mt-600 in this study may be explained by the difficulty in detection due to the size of pyridine and the reduction in interlayer spacing, which both prevent basic probes from entering the interlayer to react with unsaturated Al^{3+} ions on the layer plate.

Brønsted acid sites are mainly associated with interlayer water coordinated to exchangeable cations. In addition, H_3O^+ ions associated with negatively charged AlO_4 tetrahedra also represent Brønsted acid sites (Rupert et al. 1987). The Brønsted acidity of clay minerals generally exhibits a very sensitive dependence on the water content, which has been proposed to be influenced by the hydration of the cations (Hart and Brown 2004).The amount of interlayer water in Mt decreases after heating at 120 °C, but the polarization force of exchangeable cations becomes more concentrated in the remaining water, resulting in an increase in the proton-donating abilities of this portion of the water (Heller-Kallai 2006; Mortland and Raman 1968). After calcination at 200 °C, most interlayer water disappears, causing a reduction in the source of protons. Thus, Q_B becomes smaller. The acid sites lost at 200 °C are those that exhibit weak acid strength, which are assigned to the weakly bonded water of hydrated interlayer cations. However, the number of acid sites with higher acid strength is increased due to the enhancement of dissociation of the interlayer water, which bonds to the interlayer cations at medium strength. The Q_B of Mt-400 is much smaller because the interlayer water disappears completely, which also caused the disappearance of Brønsted acid sites in Mt-600. The detected Q_B of Mt-600 may be attributed to the water that is readsorbed on the unsaturated Al^{3+} ions produced by heating (Liu et al. 2011).

Figure 5 shows the distribution of the acid strength of Mt and its heated products. The highest-strength acid sites ($-3.0 < H_0 \leq 1.5$) exist in all products, decreasing gradually with increasing pretreatment temperature. The number of high-strength acid sites ($1.5 < H_0 \leq 3.0$) increases after heating at 120 and 200 °C, decreases at 400 °C, and disappears at 600 °C. Acid sites of medium strength ($3.3 < H_0 \leq 4.0$) do not exist in Mt, but were found when Mt was heated at 120 °C and 400 °C, respectively. After heating at 120 °C, weak acid sites with H_0 ranging from 4.0 to 4.8 significantly increase in number and disappear at 200 °C. These acid sites appear again after heating at 400 and 600 °C. Based on the above results, the characteristics of the solid acidity of Mt and its heated products are summarized in Table 3.

Solid acidity of cation-exchanged montmorillonite

Al^{3+}-Mt/Py exhibits the strongest bands at 1,540 and 1,488/cm in the DRIFT spectrum (Fig. 3d) for all of the cation-exchanged products, indicating that it contains the most abundant Brønsted acid sites and total acid sites. In contrast, Mg^{2+}-Mt/Py, Li^+-Mt/Py, Na^+-Mt/Py, and K^+-Mt/Py show little or no absorbance of Brønsted acid sites at 1,540/cm. Compared with the other cation-exchanged samples, Li^+-Mt/Py shows more intense adsorption bands for hydrogen bonds at 1,443 and 1,590/cm. A probable explanation for this phenomenon is that more residual interlayer water in the interlayer space of Li^+-Mt/Py forms hydrogen bonds with pyridine. The L:Py species of Li^+-Mt/Py may be hidden under the sharp band at 1,443/cm and is difficult to discern. Similar to the heated products, pyridine displaced water from the cation-exchanged samples, causing the reduction and broadening of the water band at 1,639/cm.

All cation-exchanged products exhibit different numbers of acid sites (Table 2; Fig. 4) and various distributions of acid strength (Fig. 6). Brønsted acids are the predominant species in Al^{3+}-Mt, whereas Na^+-Mt and K^+-Mt predominantly exhibit Lewis acidity. Mg^{2+}-Mt exhibits nearly equal numbers of Brønsted and Lewis acids as does Li^+-Mt. Al^{3+}-Mt and Mg^{2+}-Mt have larger Q_T values than Mt, reaching up to 1.20 and 1.00 mmol/g, respectively.

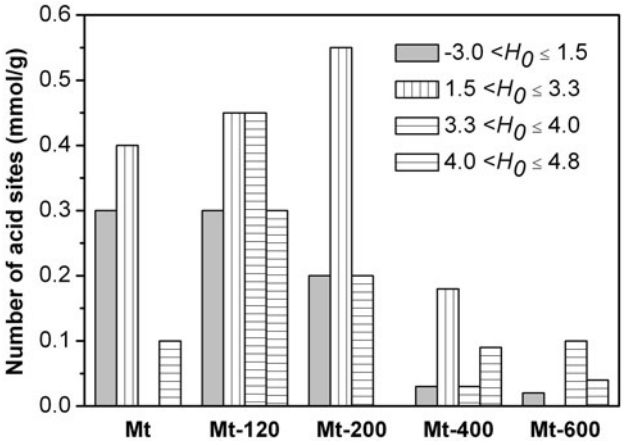

Fig. 5 Distribution of acid strength of Mt and its heated products (determined by *n*-butylamine titration in non-aqueous system)

Table 3 Characteristics of the solid acidity of Mt and its heated products

H_0	Types of solid acid sites of samples				
	Mt	Mt-120	Mt-200	Mt-400	Mt-600
−3.0–1.5	B[a] + L[b]	B + L	B + L	B + L	L
1.5–3.3	B + L	B + L	B + L	L	
3.3–4.0		B + L	B + L	L	B + L
4.0–4.8	B	B		B	B

[a] Brønsted acid sites

[b] Lewis acid sites

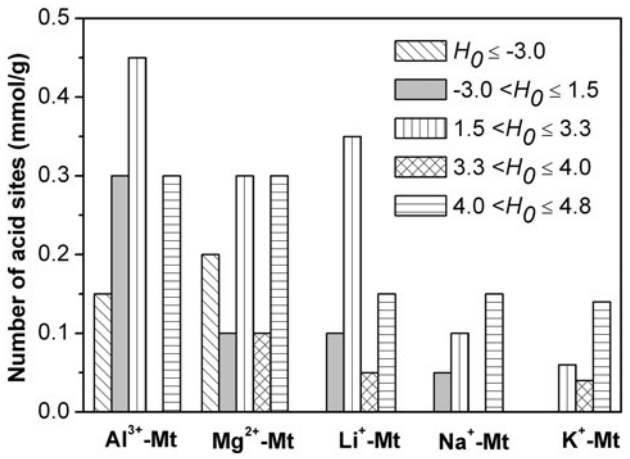

Fig. 6 Distribution of acid strength of Mt and its cation-exchanged products (determined by *n*-butylamine titration in non-aqueous system)

Monovalent cation-exchanged montmorillonite has smaller Q_T values compared with Mt. The Q_T values of all of the samples follow the order Al^{3+}-Mt > Mg^{2+}-Mt > Mt > Li^{+}-Mt > Na^{+}-Mt > K^{+}-Mt, which shows good agreement with that obtained by the NH_3-IR method (Mortland and Raman 1968) and with the order of the acid catalytic activity during the isomerization reaction (Breen and Moronta 2001) of cation-exchanged Wyoming montmorillonite. Q_B shows a similar trend. Mg^{2+}-Mt shows the highest number of Lewis acid sites (0.44 mmol/g), Li^{+}-Mt the second highest (0.38 mmol/g), and Al^{3+}-Mt the third highest (0.29 mmol/g). Na^{+}-Mt and K^{+}-Mt exhibit the smallest numbers and nearly the same Q_L. The acid strengths of Al^{3+}-Mt and Mg^{2+}-Mt are significantly higher than those of the monovalent cation-exchanged products because the acid sites with the highest acid strength ($H_0 \leq -3.0$) are observed in only Al^{3+}-Mt and Mg^{2+}-Mt. Al^{3+}-exchanged montmorillonite was found to have low Lewis acid strength by the evaluation of its Lewis acidity in the rearrangement of camphene hydrochloride into isobornyl chloride (Brown and Rhodes 1997). Thus, the acid sites with the highest acid strength presented in Al^{3+}-Mt are considered to be Brønsted acids. Li^{+}-Mt and Na^{+}-Mt exhibit an acid strength distribution ranging from −3.0 to 4.8; however, when the interlayer cation is K^{+}, only weaker-strength acid sites are present compared with those found in Mt and other cation-exchanged products (Fig. 6).

The Brønsted acidity of Mt is derived from the polarization of interlayer water molecules by interlayer-hydrated cations (Frenkel 1974; Heller-Kallai 2006; Rupert et al. 1987; Mortland and Raman 1968). The cations attract the electron pairs of the hydrated water and weaken the –OH bond in H_2O, making it easier to break. When the –OH bond breaks, a proton is released, producing a Brønsted acid. This proton-donating tendency depends on the polarizing power of the exchangeable cation, which can be quantitatively described by the cation's charge-to-radius ratios (Z/R) (Mortland and Raman 1968). The Z/R values of cations present a positive correlation with the Q_B of the corresponding cation-exchanged products (Table 2; Fig. 7). Metal cations not only behave as Brønsted acids in their hydrated form but also act as electron-pair acceptors and exhibit Lewis acidity after their hydrated water is replaced by basic probe molecules such as pyridine (Shimizu et al. 2008). Monovalent cation-exchanged products possess more Lewis acid sites than Brønsted sites because of their low content of interlayer water. Less water indicates that fewer proton sources are available to produce Brønsted acidity, which also implies the higher incidence of the complete replacement of coordinated water around the cations by pyridine. Based on the fact that all of the cation-exchanged products are originated from Mt, the numbers of Lewis acid sites associated with unsaturated Al^{3+} ions at the edge of the Mt layer in these samples are nearly equal. Thus, the observed difference in the number of Lewis acid sites of these samples should be attributed to the various types of interlayer cations in the samples. The electronegativity of the cations is used as a parameter to describe the electron-attracting ability of metal cations (Shimizu et al. 2008). The stronger the electron-attracting ability of a cation is, the higher the Lewis acidity it exhibits. The electronegativities of the cations used in the current study are shown in Fig. 7 (ionic radius and electronegativity values are on the Pauling scale). Al^{3+} exhibits the highest electronegativity, whereas Al^{3+}-Mt exhibits a relatively lower Q_L compared with that of Mg^{2+}-Mt and Li^{+}-Mt. A possible reason for this result is that the basic strength of pyridine may not be sufficiently high to react with Al^{3+}, which behaves as a very hard acid (Brown and Rhodes 1997). It is noteworthy that, in this study, *n*-butylamine titration for the determination of surface

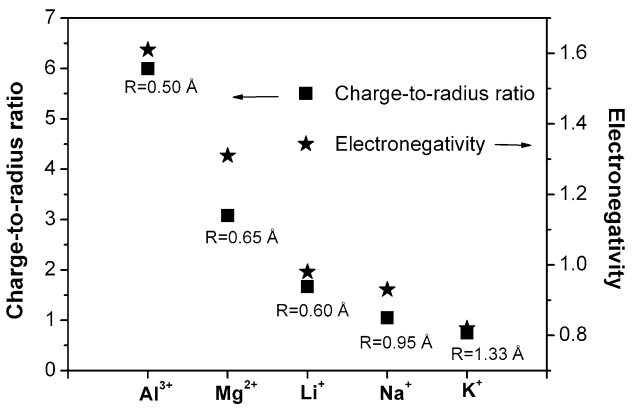

Fig. 7 The ionic radius (*R*), charge-to-radius ratio, and electronegativity of the interlayer cation

acidity was performed in non-aqueous solvents. The residual interlayer water molecules bound around exchanged cations were affected by the non-aqueous solvent and showed high dissociation degree and thus significantly contributed to the surface acidity. However, montmorillonite is a typical hydrophilic material, which usually absorbs water in the air and swells well in water. In the aqueous montmorillonite suspensions, the interlayer cations are surrounded by abundant water, and the capacity of donating protons is much lower than that in the non-aqueous solvent; thus, the interlayer water hardly shows acidity. In this case, the acidity of montmorillonite in aqueous solution and that in hydrophobic solvent is apparently different. Thus, the acidity determination results obtained in the present work mainly represent the solid acidity of montmorillonite in the special condition of non-aqueous system. The effects of some additional factors, such as humidity and temperature, on the catalytic reaction where montmorillonite was used as catalyst in aqueous environment should be taken into account.

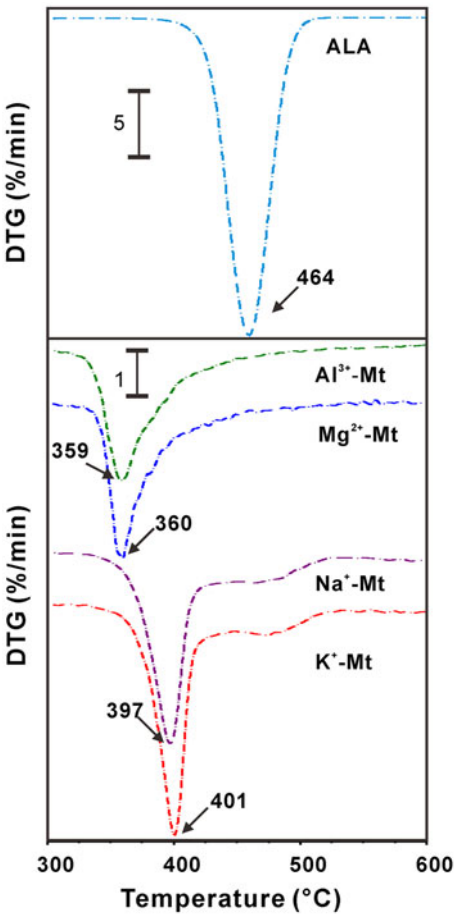

Fig. 8 The DTG curves of ALA in the absence and presence of cation-exchanged montmorillonite

Catalytic activity of cation-exchanged montmorillonite

Al^{3+}-Mt, Mg^{2+}-Mt, Na^{+}-Mt, and K^{+}-Mt were used as catalysts to investigate their catalytic activity in the thermal decomposition of ALA. ALA is decomposed at 464 °C (Fig. 8); however, ALA decomposes at a lower decomposition temperature after mixing with cation-exchanged montmorillonite. The decrease in the thermal decomposition temperature follows the order of Al^{3+}-Mt (359 °C), Mg^{2+}-Mt (360 °C), Na^{+}-Mt (397 °C), and K^{+}-Mt (401 °C), which is consistent with the order of the number of acid sites in the montmorillonite samples. This result indicates that montmorillonite exhibits catalytic activity toward the thermal decomposition of ALA and that a positive correlation exists between number of acid sites and the catalytic activity, resulting in the decrease in the thermal decomposition temperature of ALA with the increase in the number of solid acid sites of montmorillonite catalysts. However, the exact catalytic mechanism, such as the roles of Brønsted and Lewis acid sites, still needs further investigation. Because ALA could represent some types of natural organics to a certain extent, these interesting results are useful for further understanding the interaction between clay minerals and organic matter, which is very important in hydrocarbon generation.

Conclusions

Methods based on *n*-butylamine titration in non-aqueous system and DRIFT were adopted to determine the solid acidity of Mt and its modified products. All samples investigated in the current study possess both Brønsted and Lewis acid sites. Mt has many acid sites. The numbers of total, Brønsted, and Lewis acid sites are 0.80, 0.26, and 0.54 mmol/g, respectively. On heating, the number of acid sites first increases and subsequently decreases, reaching a maximum after heating to 120 °C.

Lewis acidity arises from the unsaturated Al^{3+} ions at the edges of Mt. The increased number of Lewis acid sites in Mt-120 is attributed to the loss of some absorbed water that formerly concealed the unsaturated Al^{3+} ions. The dehydroxylation event creates new Lewis acid sites at 600 °C. Difficulty in detection due to the size of pyridine molecule and the narrow interlayer space may account for the abnormally small Q_L value of Mt-400 and Mt-600. Brønsted acidity results from dissociation of the interlayer water bonded to exchangeable cations. The number of Brønsted acid sites increases at 120 °C with the increase in the proton-donating ability of the interlayer-polarized water. The acid strength of the Brønsted acid sites is related to the polarization ability of the exchangeable cation, the amount of interlayer water, and the degree of dissociation

of water coordinated to interlayer cations. The new Brønsted acid sites that appeared at 600 °C are attributed to water that has reabsorbed on the unsaturated Al^{3+} ions.

Interlayer cations behave as Brønsted acids in their hydrated form by polarizing the interlayer water and exhibiting Lewis acidity after dehydration. Brønsted acidity is predominant in Al^{3+}-Mt, whereas Na^{+}-Mt and K^{+}-Mt predominantly exhibit Lewis acidity. Mg^{2+}-Mt and Li^{+}-Mt possess approximately equal numbers of Brønsted and Lewis acid sites. Brønsted acidity shows a positive correlation with the Z/R of cations, whereas Lewis acidity depends on the electronegativity of the cations. Al^{3+}-Mt exhibits a relatively lower Q_L value because the basic strength of pyridine may not be sufficiently high to react with Al^{3+}. Cation-exchanged montmorillonite exhibited catalytic activity toward the thermal decomposition of ALA, which was positively correlated with the solid acidity of montmorillonite.

Acknowledgments This work was financially supported by the National Basic Research Program of China (Grant No. 2012CB214704-01), the National Scientific Foundation of China (No. 41272059) and the National S&T Major Project of China No. 2011ZX05008-002-21). This is a contribution (No. IS-1642) from GIGCAS.

References

Adams J, McCabe R (2006) Clay minerals as catalysts. In: Bergaya F, Theng BKG, Lagaly G (eds) Handbook of clay science, vol 1. Elsevier, Amsterdam, pp 541–581

Akçay M (2005) The surface acidity and characterization of Fe-montmorillonite probed by in situ FT-IR spectroscopy of adsorbed pyridine. Appl Catal A Gen 294(2):156–160

Arena F, Dario R, Parmaliana A (1998) A characterization study of the surface acidity of solid catalysts by temperature programmed methods. Appl Catal A Gen 170(1):127–137

Benesi H (1957) Acidity of catalyst surfaces. II. Amine titration using Hammett indicators. J Phys Chem 61(7):970–973

Bhattacharyya KG, Gupta SS (2008) Adsorption of a few heavy metals on natural and modified kaolinite and montmorillonite: a review. Adv Colloid Interface 140(2):114–131. doi:10.1016/j.cis.2007.12.008

Billingham J, Breen C, Yarwood J (1996) In situ determination of Brønsted/Lewis acidity on cation-exchanged clay mineral surfaces by ATR-IR. Clay Miner 31(4):513–522

Bjølykke K (1998) Clay mineral diagenesis in sedimentary basins–a key to the prediction of rock properties. Examples from the North Sea Basin. Clay Miner 33(1):15–34

Breen C (1991a) Thermogravimetric and infrared study of the desorption of butylamine, cyclohexylamine and pyridine from Ni-and Co-exchanged montmorillonite. Clay Miner 26(4):487–496

Breen C (1991b) Thermogravimetric study of the desorption of cyclohexylamine and pyridine from an acid-treated Wyoming bentonite. Clay Miner 26(4):473–486

Breen C, Moronta AJ (2001) Influence of exchange cation and layer charge on the isomerization of α-pinene over SWy-2, SAz-1 and Sap-Ca. Clay Miner 36(4):467–472. doi:10.1180/0009855013640001

Breen C, Deane A, Flynn J (1987) The acidity of trivalent cation-exchanged montmorillonite. Temperature-programmed desorption and infrared studies of pyridine and *n*-butylamine. Clay Miner 22(2):169–178

Brown DR, Rhodes CN (1997) Brønsted and Lewis acid catalysis with ion-exchanged clays. Catal Lett 45(1):35–40. doi:10.1023/a:1019038806333

Cseri T, Békássy S, Figueras F, Rizner S (1995) Benzylation of aromatics on ion-exchanged clays. J Mol Catal A Chem 98(2):101–107. doi:10.1016/1381-1169(95)00016-x

Dontsova KM, Norton LD, Johnston CT, Bigham JM (2004) Influence of exchangeable cations on water adsorption by soil clays. Soil Sci Soc Am J 68(4):1218–1227. doi:10.2136/sssaj2004.1218

Flessner U, Jones DJ, Rozière J, Zajac J, Storaro L, Lenarda M, Pavan M, Jiménez-López A, Rodríguez-Castellón E, Trombetta M, Busca G (2001) A study of the surface acidity of acid-treated montmorillonite clay catalysts. J Mol Catal A Chem 168(1–2):247–256. doi:10.1016/s1381-1169(00)00540-9

Frenkel M (1974) Surface acidity of montmorillonites. Clays Clay Miner 22(5–6):435–441

Fripiat J, Cruz-Cumplido M (1974) Clays as catalysts for natural processes. Annu Rev Earth Plant Sci 2:239

Geatches DL, Clark SJ, Greenwell HC (2010) Role of clay minerals in oil-forming reactions. J Phys Chem A 114(10):3569–3575. doi:10.1021/jp9096869

Hart MP, Brown DR (2004) Surface acidities and catalytic activities of acid-activated clays. J Mol Catal A Chem 212(1–2):315–321. doi:10.1016/j.molcata.2003.11.013

He H, Yang D, Yuan P, Shen W, Frost RL (2006) A novel organoclay with antibacterial activity prepared from montmorillonite and Chlorhexidini Acetas. J Colloid Interface Sci 297(1):235–243. doi:10.1016/j.jcis.2005.10.031

Heller-Kallai L (2006) Thermally modified clay minerals. In: Bergaya F, Theng BKG, Lagaly G (eds) Handbook of clay science, vol 1. Elsevier, Amsterdam, pp 289–308

Hetényi M (1995) Simulated thermal maturation of type I and III kerogens in the presence, and absence, of calcite and montmorillonite. Org Geochem 23(2):121–127. doi:10.1016/0146-6380(94)00120-p

Jankovič Ľ, Komadel P (2003) Metal cation-exchanged montmorillonite catalyzed protection of aromatic aldehydes with Ac_2O. J Catal 218(1):227–233. doi:10.1016/s0021-9517(03)00138-6

Jerónimo D, Guil JM, Corbella BM, Vasques H, Miranda A, Silva JM, Lobato A, Pires J, Carvalho AP (2007) Acidity characterization of pillared clays through microcalorimetric measurements and catalytic ethylbenzene test reaction. Appl Catal A Gen 330:89–95. doi:10.1016/j.apcata.2007.07.013

Johns WD (1979) Clay mineral catalysis and petroleum generation. Annu Rev Earth Plant Sci 7:183

Johns WD, Shimoyama A (1972) Clay minerals and petroleum-forming reactions during burial and diagenesis. AAPG Bull 56(11):2160–2167

Khaorapapong N, Ontam A, Youngme S, Ogawa M (2008) Solid-state intercalation and in situ formation of cadmium sulfide in the interlayer space of montmorillonite. J Phys Chem Solids 69(5–6):1107–1111

Larter SR, Douglas AG (1982) Pyrolysis methods in organic geochemistry: an overview. J Anal Appl Pyrol 4(1):1–19. doi:10.1016/0165-2370(82)80023-5

Liu D, Yuan P, Liu H, Cai J, Qin Z, Tan D, Zhou Q, He H, Zhu J (2011) Influence of heating on the solid acidity of montmorillonite: a combined study by DRIFT and Hammett indicators. Appl Clay Sci 52(4):358–363. doi:10.1016/j.clay.2011.03.016

Madejová J, Komadel P (2001) Baseline studies of the clay minerals society source clays: infrared methods. Clays Clay Miner 49(5):410–432

Mahmoud S, Hammoudeh A, Al-Noaimi M (2003) Pretreatment effects on the catalytic activity of Jordanian bentonite. Clays Clay Miner 51(1):52–57. doi:10.1346/ccmn.2003.510106

Mortland M, Raman K (1968) Surface acidity of smectites in relation to hydration, exchangeable cation, and structure. Clays Clay Miner 16(5):393–398

Motokura K, Nakagiri N, Mizugaki T, Ebitani K, Kaneda K (2007) Nucleophilic substitution reactions of alcohols with use of montmorillonite catalysts as solid Brønsted acids. J Org Chem 72(16):6006–6015. doi:10.1021/jo070416w

Noyan H, Önal M, Sarikaya Y (2006) The effect of heating on the surface area, porosity and surface acidity of a bentonite. Clays Clay Miner 54(3):375–381. doi:10.1346/ccmn.2006.0540308

Reddy CR, Iyengar P, Nagendrappa G, Jai Prakash BS (2005) Esterification of succinic anhydride to di-(p-cresyl) succinate over Mn + -montmorillonite clay catalysts. J Mol Catal A Chem 229(1–2):31–37. doi:10.1016/j.molcata.2004.10.044

Reddy CR, Nagendrappa G, Jai Prakash BS (2007) Surface acidity study of Mn + -montmorillonite clay catalysts by FT-IR spectroscopy: correlation with esterification activity. Catal Commun 8(3):241–246

Reddy CR, Bhat YS, Nagendrappa G, Jai Prakash BS (2009) Brønsted and Lewis acidity of modified montmorillonite clay catalysts determined by FT-IR spectroscopy. Catal Today 141(1–2):157–160

Rupert JP, Granquist WT, Pinnavaia TJ (1987) Catalytic properties of clay minerals. Chemistry of clays and clay minerals. Longman scientific and technical, New York

Shimizu K-i, Higuchi T, Takasugi E, Hatamachi T, Kodama T, Satsuma A (2008) Characterization of Lewis acidity of cation-exchanged montmorillonite K-10 clay as effective heterogeneous catalyst for acetylation of alcohol. J Mol Catal A Chem 284(1–2):89–96. doi:10.1016/j.molcata.2008.01.013

Singh B, Patial J, Sharma P, Agarwal SG, Qazi GN, Maity S (2007) Influence of acidity of montmorillonite and modified montmorillonite clay minerals for the conversion of longifolene to isolongifolene. J Mol Catal A Chem 266(1–2):215–220

Tyagi B, Chudasama CD, Jasra RV (2006) Characterization of surface acidity of an acid montmorillonite activated with hydrothermal, ultrasonic and microwave techniques. Appl Clay Sci 31(1–2):16–28

Ursu AV, Jinescu G, Gros F, Nistor ID, Miron ND, Lisa G, Silion M, Djelveh G, Azzouz A (2011) Thermal and chemical stability of Romanian bentonite. J Therm Anal Calorim 106(3):965–971. doi:10.1007/s10973-011-1414-z

Vaccari A (1999) Clays and catalysis: a promising future. Appl Clay Sci 14(4):161–198

Varma RS (2002) Clay and clay-supported reagents in organic synthesis. Tetrahedron 58(7):1235–1255

Walling C (1950) The acid strength of surfaces. J Am Chem Soc 72(3):1164–1168

Wattel-Koekkoek EJW, van Genuchten PPL, Buurman P, van Lagen B (2001) Amount and composition of clay-associated soil organic matter in a range of kaolinitic and smectitic soils. Geoderma 99(1–2):27–49. doi:10.1016/s0016-7061(00)00062-8

Zheng Y, Zaoui A, Shahrour I (2010) Evolution of the interlayer space of hydrated montmorillonite as a function of temperature. Am Mineral 95(10):1493–1499. doi:10.2138/am.2010.3541

Zhou CH (2011) Clay mineral-based catalysts and catalysis. Appl Clay Sci 53(2):85